AIAA SciTech Forum
8–12 January 2018, Kissimmee, Florida
2018 AIAA Aerospace Sciences Meeting

10.2514/6.2018-0577

Thermal Control of Vortex-induced Vibration of Two Tandem Cylinders

Hui Wan[a], Soumya S. Patnaik[b]

[a]Department of Mechanical and Aerospace Engineering, University of Colorado, Colorado Springs, CO 80918, USA, hwan@uccs.edu

[b]Power and Control Division, Aerospace Systems Directorate, Air Force Research Laboratory, WPAFB, OH 45433, USA, *soumya.patnaik.1@us.af.mil*

Nomenclature

D	characteristic length; cylinder diameter	t	non-dimensional time
f	natural frequency of structure	$\mathbf{u}$	velocity vector
$\mathbf{g}$	gravity acceleration	U_{red}	Reduced velocity
M_{red}	Reduced mass	*Greek symbols*	
p	pressure	β	thermal expansion coefficient (1/K)
Pr	Prandtl number (7.1 for water)	κ	thermal diffusivity (m^2/s)
Q	body motion displacement	ν	kinematic viscosity (m^2/s)
Re	Reynolds number	$\Delta\theta$	temperature difference between cylinder and upcoming flow
Ri	Richardson number	θ	temperature
S	Center-to-center distance between two bodies		

1. Introduction

The suppression of vortex-induced vibration (VIV) is of practical interest to many engineering fields. Methods such as surface protrusion, shrouds, near wake stabilizers, and tripping wires have been discussed [1-3]. Recently, we have used thermal control to suppress the VIV of a single body [6]. The thermal control parameter *Ri* characterizes the ratio between the thermal induced buoyancy force and the inertial force. The amplitude of VIV can even be fully suppressed when *Ri* is above a critical value. It is also found that for a flexible body, drag gradually increases with the Richardson number. A drag reduction of 30-40% can be obtained at the critical Richardson number.

In this current paper, we have extended our previous study to investigate the suppression of vortex-induced vibration of two tandem cylinders placed in serial. Here we combine thermal control and near wake stabilizers. Two cylinders separated with a distance *S* were aligned along the direction of the thermal induced buoyancy force. When the distance is small, the vortex shedding of the first cylinder is disturbed due to proximity effect and its VIV is reduced. We then use thermal control to suppress the vibration of the second cylinder. Hence, by applying thermal energy to only one body, the VIV of both bodies was suppressed. This method can also be extended to reduce the VIV of multiple bodies placed in serial.

2. Mathematical formulation

Using incompressible flow and Boussinesq approximation, the non-dimensional Navier-Stokes equation and thermal equation can be expressed as:

$$\nabla \cdot \mathbf{u} = 0 \tag{1}$$

$$\frac{\partial \mathbf{u}}{\partial t} + \mathbf{u} \cdot \nabla \mathbf{u} = -\nabla p + \frac{1}{Re}\nabla^2 \mathbf{u} + Ri\theta \tag{2}$$

$$\frac{\partial \theta}{\partial t} + \mathbf{u} \cdot \nabla \theta = \frac{1}{RePr}\nabla^2 \theta \tag{3}$$

in which the Reynolds number Re $(= UD/\nu)$, is the ratio of the inertial force to the viscous force. The diameter of the cylinder D was taken as the characteristic length, and the free stream velocity U as the characteristic velocity. The fluid properties thermal diffusivity, kinematic viscosity, and thermal expansion coefficient are denoted by κ, ν, and β, respectively. The Prandtl number Pr $(= \nu/\kappa)$ is the ratio of the kinematic to the thermal diffusivity and is a property of the fluid medium. In this study, water is taken as the fluid medium, and its Prandtl number is 7.1. The Richardson number Ri $(= g\beta\Delta\theta D/U^2)$ characterizes the buoyancy force and the inertial force. When the heat transfer between the cylinder and the fluid medium is dominated by forced convection, the Richardson number is far below unity, i.e., $Ri \ll 1$. Whereas, when natural convection dominates heat transfer, $Ri \gg 1$. The term $RePr$ in equation (3) can also be written as the Peclet number Pe $(= RePr)$. The velocity boundary condition on the cylinder surface in our study is non-slip and impermeable, i.e. $\mathbf{u} = 0$. The temperature of the cylinder and the upcoming flow are set to 1 and 0, respectively.

The general equation of motion of an elastically mounted cylinder is as follows:

$$m\frac{\partial^2 Q_i}{\partial t^2} + c\frac{\partial Q_i}{\partial t} + kQ_i = F_i \tag{4}$$

The non-dimensional equation of body motion is then:

$$\frac{\partial^2 Q_i}{\partial t^2} + \frac{4\pi\zeta}{U_{red}}\frac{\partial Q_i}{\partial t} + \frac{4\pi^2}{U_{red}^2}Q_i = \frac{1}{2M_{red}}C_i \tag{5}$$

in which the reduced velocity U_{red} is defined as $U_{red}=\frac{U}{fD}$, and the reduced mass $M_{red}=\frac{m}{\rho_f D^2}$. The natural frequency of the cylinder is denoted by f. The subscript *'i'* stands for the motion direction. The structure is getting more flexible, and the natural frequency of its vibration is smaller with increase in the reduced velocity. C_i represents the hydrodynamic force coefficient in the body motion. The damping coefficient c or ζ is set to be zero in the current study. The Navier-Stokes equations and the body motion equation are coupled in a similar way as that in previous studies [6-8].

3. Problem description and numerical method

3.1. Problem description

The problem in this study is illustrated in Fig. 1, in which two cylinders with a distance S apart were aligned with the direction of buoyancy force. Fluid flows past the bodies from the bottom to the top. The flow direction and the thermal induced buoyancy force were aligned to take full advantage of the thermal effects. The two bodies were elastically mounted with one degree of freedom in the horizontal direction. When the flow passes a cylinder kept at elevated temperature, mixed-convection occurs, involving both natural and forced convection. The relative importance of natural convection and forced convection is characterized by the Richardson number.

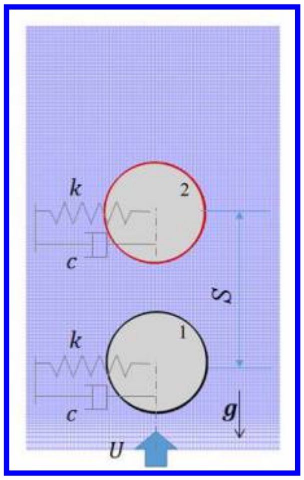

Fig. 1. Mesh and configuration of the two bodies. The flow was from the bottom to the top. Each of the two bodies was elastically mounted with one degree of freedom in horizontal direction. The vortex shedding of first body can be disturbed by the second body; while the vortex shedding of the second body can be reduced by thermal control.

3.2. Numerical method

The Navier-Stokes equations were discretized using a cell-centered, collocated arrangement of the primitive variables $(\mathbf{u}, p)$ and integrated in time using fractional step method [9]. Second-order central difference schemes in space were employed to both convection and diffusion terms in momentum and temperature equations. There are also many related validations in our previous study[6].

4. **Results and discussions**

In this study, we consider a cylinder that can freely oscillate in the x-direction. Its degree of freedom in y-direction is fixed. Flow passes through the cylinder from the bottom to the top, and the cylinder is subject to vibration when vortices are generated and shed periodically. The cylinder is heated, and the thermal effects on the vortex-induced vibration is studied. The Reynolds number is 150, and the reduced mass M_{red} is 2.0 throughout this study.

4.1 Single body vibration at $U_{red} = 4.0$, Ri = 0

We consider pure forced convection first, i.e., Ri = 0. This simulation is essentially same as the previous validation case. Fig. 2a shows the oscillation in the periodic states. Fig. 2b shows the vortex structure, characterized by two-column vortex shedding. The time averaged drag coefficient C_Y (in y-direction) is 2.37 in our previous study[6].

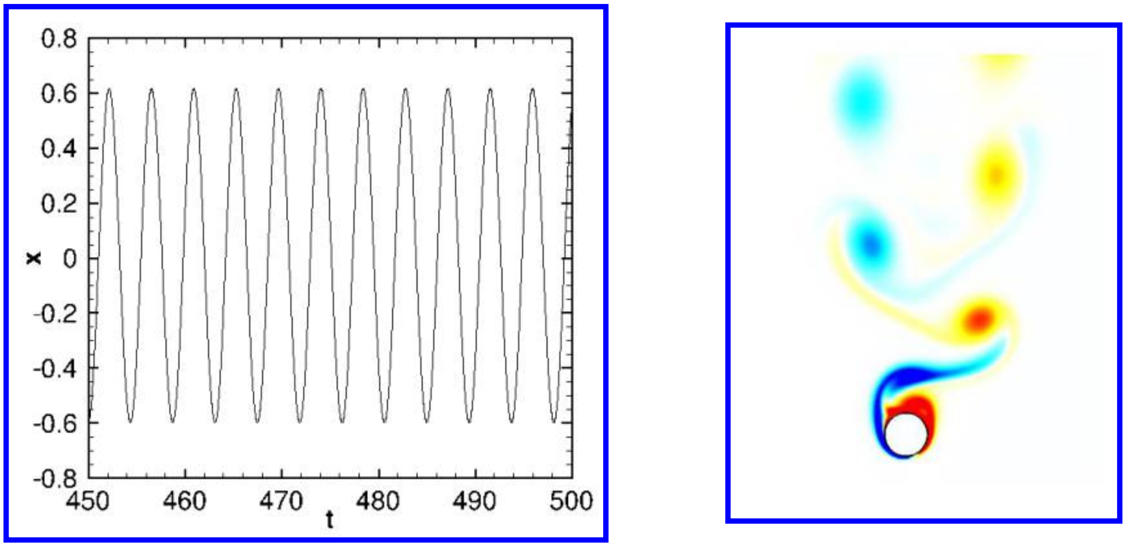

(a) Steady phase (b) Steady phase

Fig. 2. Time history of the displacement of cross-stream vibration, $U_{red} = 4.0$, Ri = 0.

4.2 Two bodies 3D apart

Now we study the case in which the distance between the two cylinders is 3D, i.e. the center-to-center distance is three diameters of the cylinder. The temperature and vorticity field are shown in Fig. 3. Vortices are shed from both of the two cylinders. Figure 4 presents the time history of the displacement and the force coefficient. It can be seen that the vibration of the first cylinder is quite small (actually its vibration amplitude is around 0.0035). The vibration of the second cylinder is 0.28, which is about one-half of the vibration of single cylinder, as shown in section 4.1.

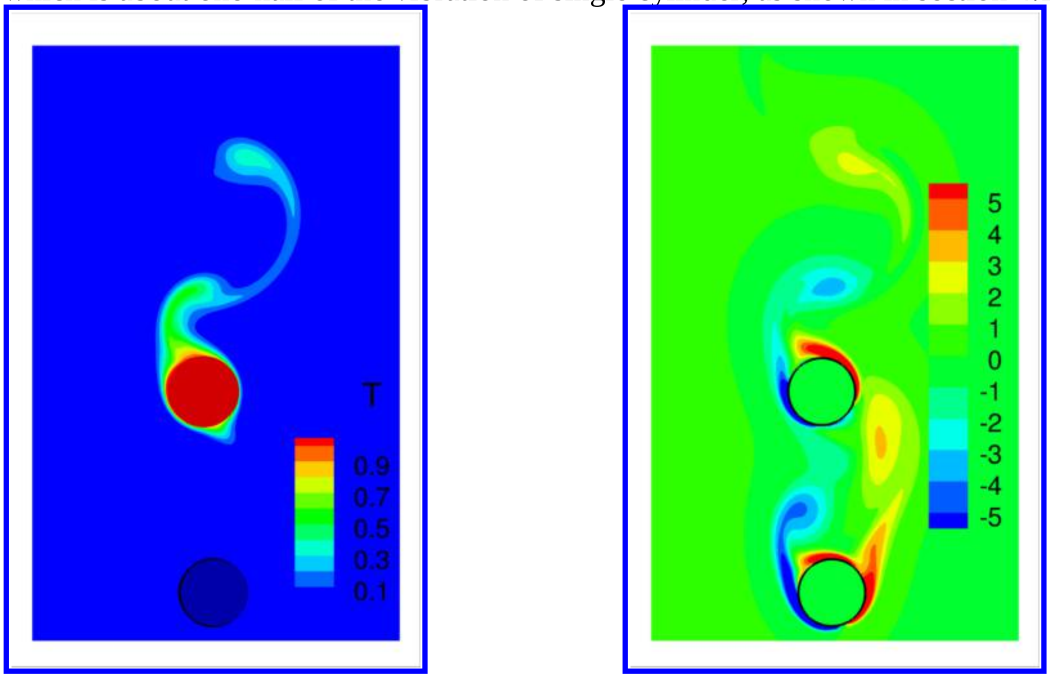

(a) Temperature (b) Vorticity

Fig. 3. Temperature and flow field, $U_{red} = 4.0$, *Ri* = 1.0 on the second body, *S* = 3D.

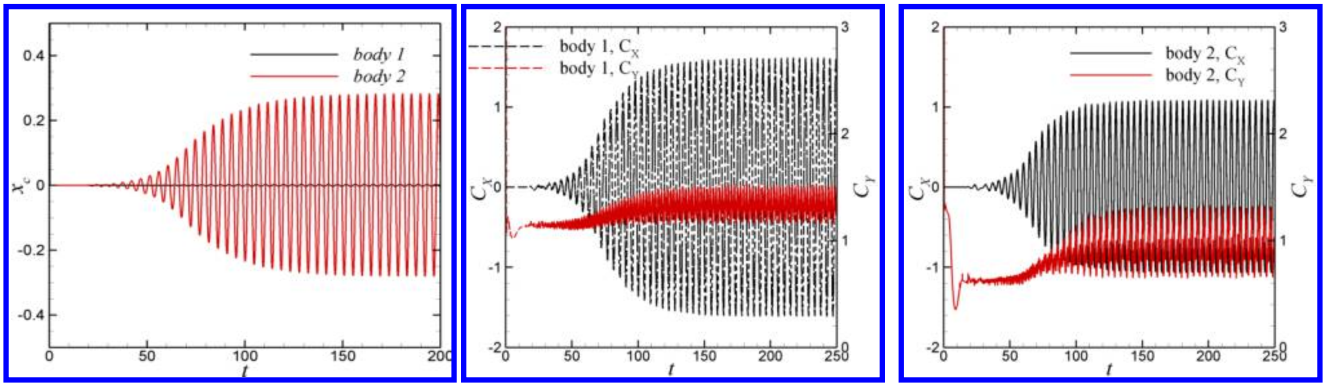

Fig. 4. Time history of the displacement of cross-stream vibration, force coefficients, $U_{red} = 4.0$, *Ri* = 1.0 on the second body, *S* = 3D.

4.3 Two bodies 2D apart

As the distance between the two cylinder is reduced to 2D, the vortex structure behind the first (front) cylinder is almost symmetric. There is no enough space for the vortex forming in the backside of the first body. The vortex shedding of the second cylinder is also suppressed due to the thermal effect (as shown in Fig. 5). From Fig. 6, we can see that the first cylinder keeps stationary, and the vibration amplitude of the second cylinder is around 0.015, i.e. 1.5% of the diameter of the cylinder. The time-averaged drag coefficient of the first and the second cylinder is around 1.22 and 0.49, respectively (Fig.6).

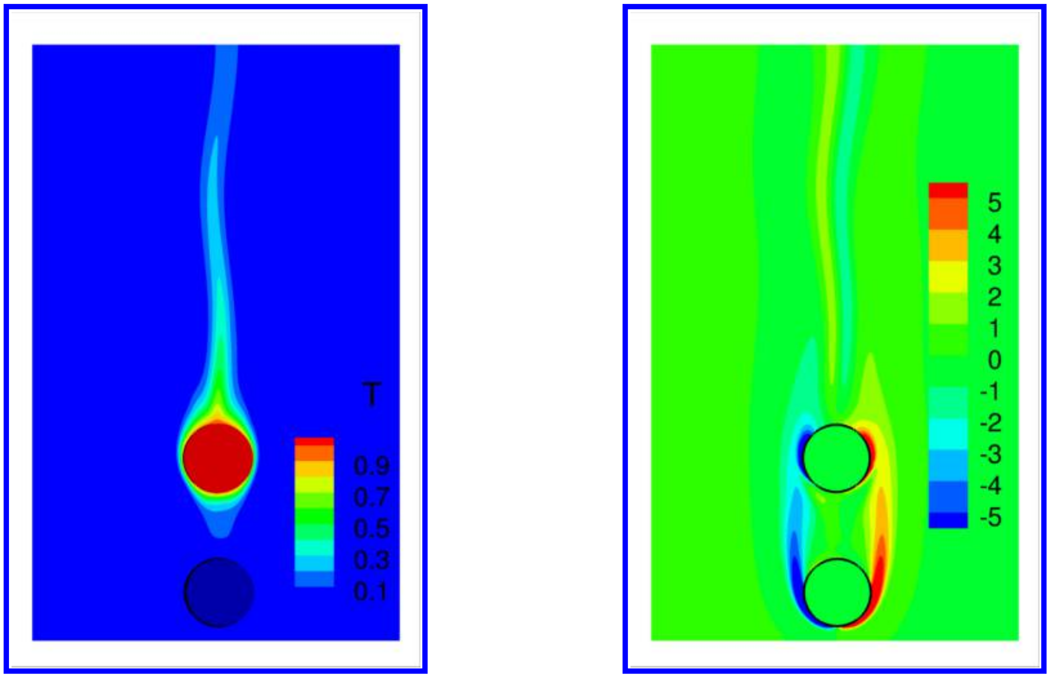

(a) Temperature (b) Vorticity

Fig. 5. Temperature and vorticity field, $U_{red} = 4.0$, *Ri* = 1.0 on the second body, the distance between the two bodies is 2D.

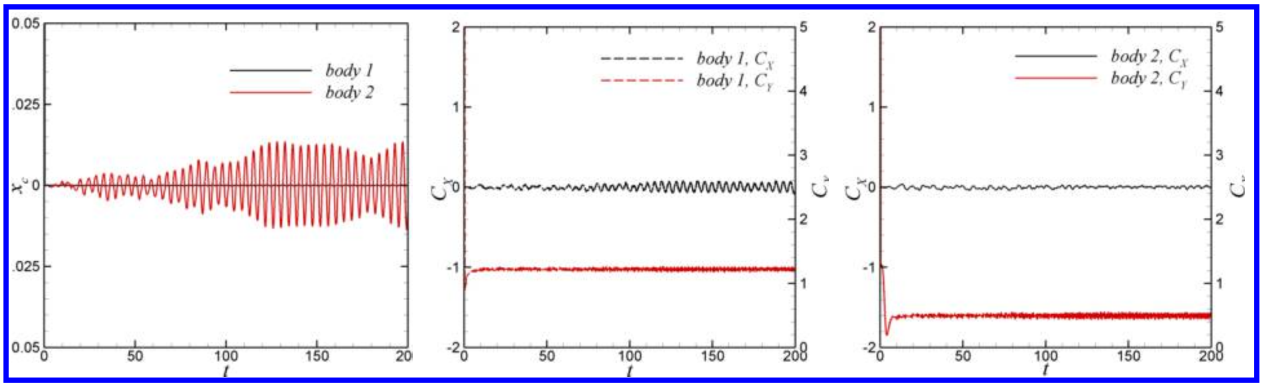

Fig. 6. Time history of the displacement of cross-stream vibration, force coefficients, $U_{red} = 4.0$, *Ri* = 1.0 on the second body, *S* = 2D.

4.4 Two bodies 1.5 D apart, Ri = 1.0

Figure 7 shows the temperature and vorticity field when the distance of the two bodies is 1.5D, and the Richardson number is 1.0. It can be seen that the vortex shedding of the first body is suppressed due to the proximity between the two bodies. The second body, as usual, do not generate vortex shedding due to the thermal control. The first cylinder (body 1 in the figure) literally shows no vibration, and the vibration amplitude of the second cylinder is less than 1% (Fig. 8). The time-averaged drag coefficient ($\overline{C_Y}$) experienced by the first and the second bodies are 1.27 and 0.38, respectively.

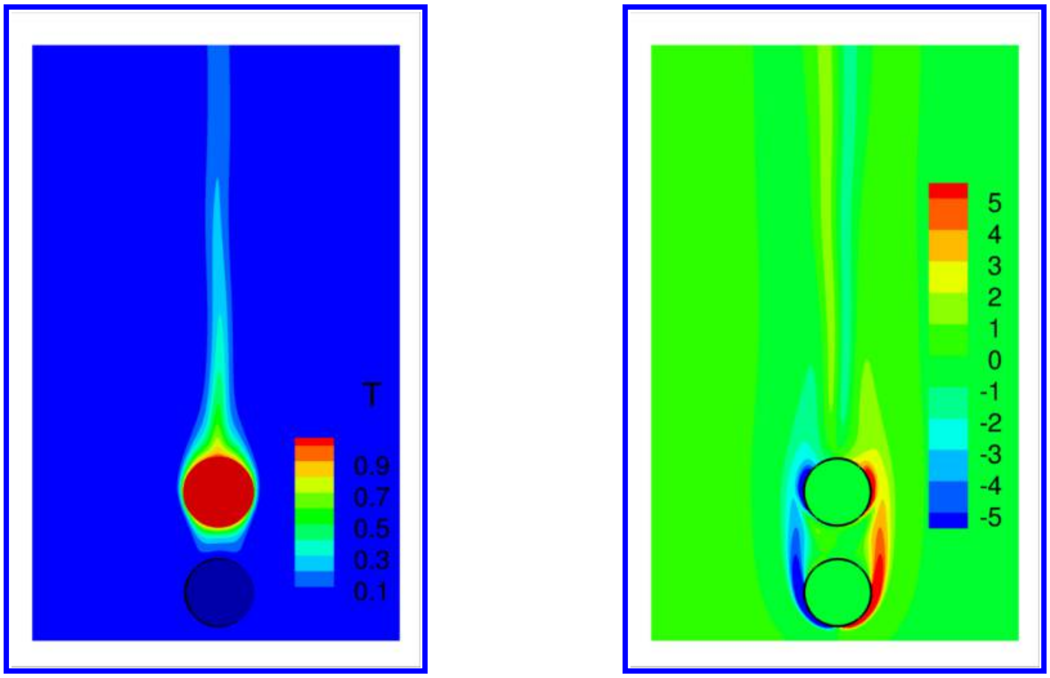

(a) Temperature (b) Vorticity

Fig. 7. Temperature and flow field, $U_{red} = 4.0$, *Ri* = 1.0 on the second body, *S* = 1.5D.

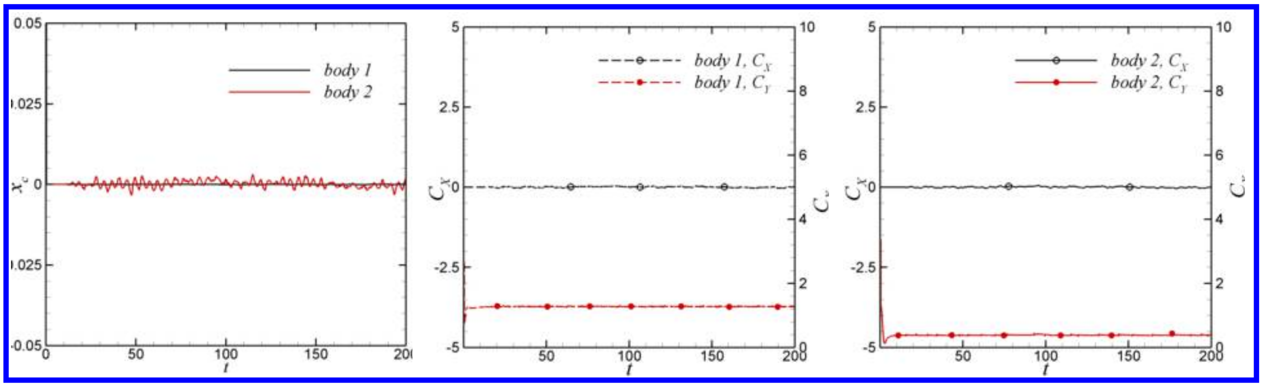

Fig. 8. Time history of the displacement of cross-stream vibration, force coefficients, $U_{red} = 4.0$, *Ri* = 1.0 on the second body, *S* = 1.5D.

4.5 Two bodies 1.5 D apart, Ri = 0.5

In the previous section, we have seen that when the body separation is 1.5D, the vibration of the two bodies are suppressed when Ri = 1.0. The question is, in a small separation such as 1.5D, can a smaller Richardson number be used to suppress the vibration? Therefore, we further numerically tested Ri = 0.5 and separation 1.5D. The simulated results till the non-dimensional time t = 300 are shown in Fig.9, in which the body 1 basically undergoes negligible vibration (Fig. 9a). The vibration amplitude of the body 2 is around 0.007. The time-averaged drag coefficient $\overline{C_Y}$ is 1.22 and 0.16, respectively for the first and the second bodies.

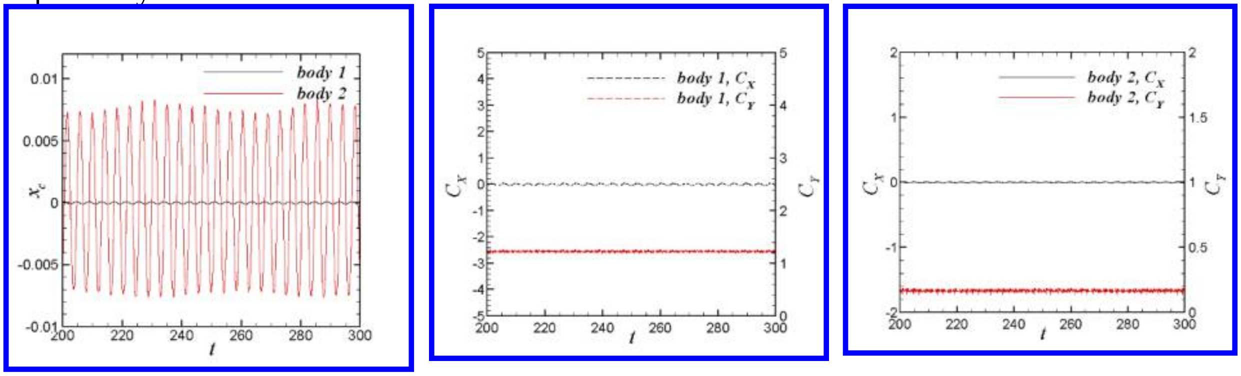

Fig. 9. Time history of the displacement of cross-stream vibration, force coefficients, $U_{red} = 4.0$, *Ri* = 0.5 on the second body, *S* = 1.5D.

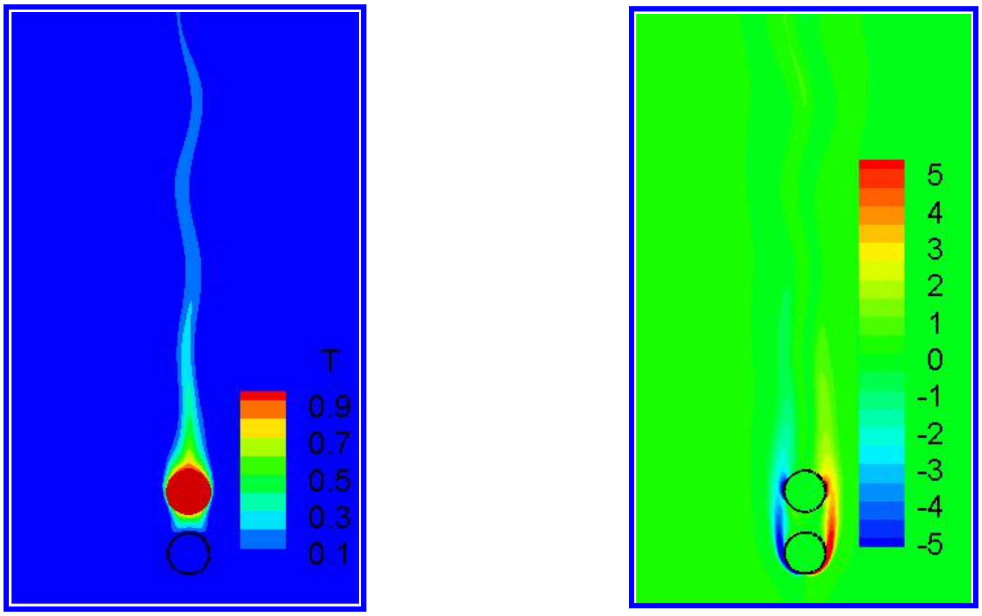

(a) Temperature

(b) Vorticity

Fig. 10. Temperature and flow field, $U_{red} = 4.0$, *Ri* = 0.5 on the second body, *S* = 1.5D.

The temperature field and flow structure at t = 300 are shown in Fig. 10. The vortex structure is basically symmetric along the center line of the two bodies, and there is no vortex shedding occurs. The temperature contour shows wiggling of the wake, indicating small force oscillations from the second body, which is consistent with the small oscillations in the force coefficient C_X in Fig. 9.

5. Conclusion

In this work, the vortex-induced vibration of two tandem cylinders were numerically studied. The two cylinders were elastically mounted with one degree of freedom in horizontal direction. The Reynolds number and the reduced mass considered in this study were 150 and 2.0, respectively. The second cylinder was heated and the distance between the two cylinders was varied to study the suppression of the two cylinders. It has been found that one heated cylinder can be used to reduce the vibration of the two cylinders, once the distance is small enough, e.g. 2D. The suppression of vortex shedding of the front and back cylinders is due to the proximity effect and the thermal effects, respectively. Also, when the two cylinder gets further closer (e.g. 1.5D), less thermal control, i.e. smaller Ri, is needed to suppress the VIV of the two bodies. This method may also be extended to the VIV suppression of multiple bodies.

Acknowledgements

The Authors gratefully acknowledge financial support from AFRL/RQQI under contract No. FA8650-04-D-2404 and the Air Force Research Laboratory DoD Supercomputing Resource Center for computing time and resources.

Reference

1. Zdravkovich, M. M. "Review and classification of various aerodynamic and hydrodynamic means for suppressing vortex shedding " *Journal of Wind Engineering and Industrial Aerodynamics* Vol. 7, No. 2, 1981, pp. 145-189.doi: 10.1016/0167-6105(81)90036-2
2. Sarpkaya, T. "A critical review of the intrinsic nature of vortex-induced vibrations," *Journal of Fluids and Structures* Vol. 19, No. 4, 2004, pp. 389-447.
3. Hover, F. S., Tvedt, H., and Triantafyllou, M. S. "Vortex-induced vibrations of a cylinder with tripping wires," *Journal of Fluid Mechanics* Vol. 448, 2001, pp. 175-195.
4. Kwon, K., and Choi, H. "Control of laminar vortex shedding behind a circular cylinder using splitter plates. ," *Physics of Fluids* Vol. 8, 1996, pp. 479-486.
5. Strykowski, P. J., and Sreenivasan, K. R. "On the formation and suppression of vortex ‘shedding’ at low Reynolds numbers," *Journal of Fluid Mechanics* Vol. 218, 1990, pp. 71-107.
6. Wan, H., and Patnaik, S. S. "Suppression of vortex-induced vibration of a circular cylinder using thermal effects," *Physics of Fluids* Vol. 28, No. 12, 2016.doi: 12360310.1063/1.4972178
7. Wan, H., Dong, H., and Liang, Z. "Vortex Formation of Freely Falling Plates," *50th AIAA Aerospace Sciences Meeting including the New Horizons Forum and Aerospace Exposition*. Nashville, Tennessee, 2011.
8. Wan, H., Dong, H. B., and Huang, G. P. "Hovering Hinge-Connected Flapping Plate with Passive Deflection," *AIAA Journal* Vol. 50, No. 9, 2012, pp. 2020-2027.doi: Doi 10.2514/1.J051375
9. Mittal, R., Dong, H., Bozkurttas, M., Najjar, F. M., Vargas, A., and von Loebbecke, A. "A versatile sharp interface immersed boundary method for incompressible flows with complex boundaries," *Journal of Computational Physics* Vol. 227, No. 10, 2008, pp. 4825-4852.doi: DOI 10.1016/j.jcp.2008.01.028